

DISTILLING WITH RESIDUAL NETWORK FOR SINGLE IMAGE SUPER RESOLUTION

Xiaopeng Sun, Wen Lu, Rui Wang, Furui Bai

School of Electronic Engineering, Xidian University, Xi'an, China
 xpsun@stu.xidian.edu.cn, luwen@mail.xidian.edu.cn, {wangrui, frbai}@stu.xidian.edu.cn

ABSTRACT

Recently, the deep convolutional neural network (CNN) has made remarkable progress in single image super resolution (SISR). However, blindly using the residual structure and dense structure to extract features from LR images, can cause the network to be bloated and difficult to train. To address these problems, we propose a simple and efficient distilling with residual network (DRN) for SISR. In detail, we propose residual distilling block (RDB) containing two branches, while one branch performs a residual operation and the other branch distills effective information. To further improve efficiency, we design residual distilling group (RDG) by stacking some RDBs and one long skip connection, which can effectively extract local features and fuse them with global features. These efficient features beneficially contribute to image reconstruction. Experiments on benchmark datasets demonstrate that our DRN is superior to the state-of-the-art methods, specifically has a better trade-off between performance and model size.

Index Terms— Super resolution, convolutional neural network, distilling with residual network

1. INTRODUCTION

The task of super-resolution (SR) is to reconstruct a high-resolution (HR) image consistent with it from a low-resolution (LR) image. The tasks of super-resolution are quite extensive, such as in the field of video surveillance, medical imaging, and target detection. However, SR is a reverse process of information loss. LR images have abundant low-frequency information but lose high-frequency information only in HR images. In order to address these problems, plenty of learning based methods have been applied to learn a mapping between HR images and LR images pairs.

Recently, Convolutional neural networks (CNN) are applied to a large number of visual tasks, including SR, which

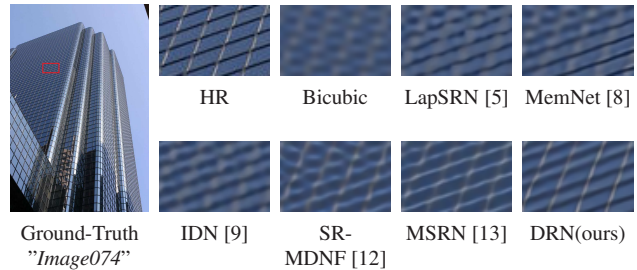


Fig. 1: Subjective quality assessment for 4× upscaling on the general image: *Image074* from Urban100.

achieves better results than traditional methods. Dong et al. [1] firstly proposed SRCNN by a fully convolutional neural network, which could learn an end-to-end mapping between LR images and HR images, and made significant improvement over the conventional method (such as A+ [2]) with only three layers. Later, Kim et al. [3] proposed VDSR increasing depth to 20 and made significant progress over SRCNN. Then, the DRCN Kim et al. [4] proposed relieved the difficulty of deep network training by using gradient clips, skipping connections and recursive supervision. Lai et al. [5] proposed LapSRN that consisted of a deep laplacian pyramid, which reconstructed the HR image by step by step amplification. Based on ResNet [6], Lim et al. [7] designed a very deep and wide network EDSR. Tai et al. proposed MemNet [8] consisted of memory blocks, but increased the computational complexity. Hui et al. proposed IDN [9] reducing model computational complexity by distillation model. But IDN's distillation operation has the problem of information loss. Based on the full integration of densenet and resnet, Yulun et al. proposed RDN [10], which achieved quite outstanding results. Later, Yulun et al. introduced the attention mechanism to propose RCAN [11], and achieved amazing achievements. But these two models are too complicated, and the amount of parameters is huge. For the purpose of using different receptive fields to extract information while reducing model complexity, Li et al. proposed MSRN [13] utilizing 3×3 and 5×5 convolutional kernel to fuse features. Although they have achieved the goal of optimizing the model, the experimental results are not outstanding enough. Their structure over-reuses features, causing the network structure to become

This research was supported in part by the National Natural Science Foundation of China (Grant Nos. 61432014, 61871311, 61876146), the National Key Research and Development Program of China (Grant No. 2016QY01W0200), the Key Industrial Innovation Chain Project in Industrial Domain (Grant No. 2016KTZDGY04-02), National High-Level Talents Special Support Program (Leading Talent of Technological Innovation of Ten-Thousands Talents Program)(Grant No. cs31117200001).

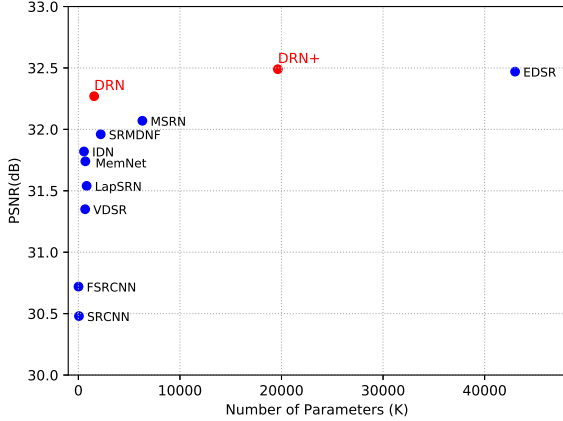


Fig. 2: Performance and number of parameters. Results are evaluated on Set5(4×). Our models have a better trade-off between performance and model size.

bloated and difficult to train.

To address these problems, we propose a simple and efficient distilling with residual network for SISR. As shown in Fig3, residual distilling group(RDG) is proposed as the building module for DRN. As Fig.4 shows, we stack several residual distilling blocks(RDB) with one long skip connection(LSC) in each RDG. These long memory connections in RDBs bypass rich low-frequency information, which simplifies the flow of information. The output of one RDB can directly access each layer of the next RDB, resulting in continuous feature transfer. In addition, we introduced a convolutional layer with a 1×1 kernel as feature fusion and dimensionality reduction at the last position of the RDB. The residual distilling operation is in each RDB and consists of 1×1 , 3×3 and 1×1 convolution kernels. The output of the sum of RDG and the global residual learning is sent to image reconstruction by pixelshuffle [14]. In summary, our main contributions are three-fold:

- We propose residual distilling block(RDB), which enjoys benefits from ResNet [6] and distills efficient information. It can fuse common feature while maintaining the ability to distill important features. Different from IDN [9], our RDB using residual distilling structure, retains as much information.
- Our method has few network parameters and a simple network structure, which is easy to recurrent. It is a compact network with a significant trade-off between performance and model size.
- We propose a simple and efficient distilling with residual network(DRN) for high-quality image SR. What's more, it is easy to understand and better than most of the state-of-the-art methods.

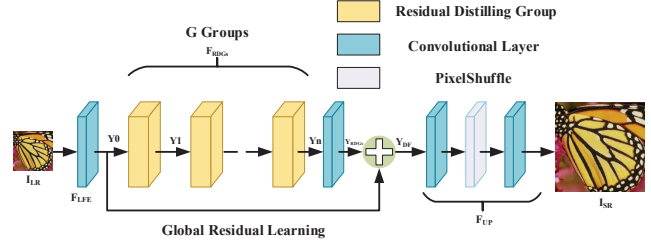


Fig. 3: Distilling with Residual Network Network(DRN).

2. DISTILLING WITH RESIDUAL NETWORK

2.1. Network Architecture

As shown in Fig.3, the proposed DRN mainly consists three parts: low-level feature extraction(LFE), residual distilling groups(RDGs), image reconstruction(IR). Here, let's denote I_{LR} and I_{HR} as the input and output of DRN. As referred in [15, 7, 11], one convolutional layer is suitable to extract the low-level feature Y_0 from the input LR

$$Y_0 = F_{LFE}(I_{LR}), \quad (1)$$

where F_{LFE} represents convolutional function. Y_0 is then sent to the residual distilling groups and used for global residual learning. Furthermore, we can have Y_{RDGs} that's the output of GDGs

$$Y_{RDGs} = F_{RDGs}(Y_0), \quad (2)$$

where F_{RDGs} denotes the operations of the RDGs we proposed, which contains G groups. With the deep feature information being extracted by a set of RDGs, we can further fuse the features, which contains global residual learning and Y_{RDGs} . So, we have all the features extracted Y_{DF} ,

$$Y_{DF} = Y_0 + Y_{RDGs}. \quad (3)$$

Then Y_{DF} is upscaled through image reconstruction module. We can get upscaled feature Y_{UP}

$$Y_{UP} = F_{UP}(Y_{DF}), \quad (4)$$

where F_{UP} denotes the image reconstruction module. Then the upscaled feature is reconstructed by one convolution layer. In general, the overall process can be expressed as

$$I_{SR} = F_{IR}(F_{UP}) = F_{IR}(F_{RDGs}(F_{LFE}(I_{LR}))), \quad (5)$$

where F_{IR} and F_{RDGs} denote the image reconstruction and the function of our RDGs respectively.

2.2. Residual Distilling Group

We now give more details about RDG. Through Fig.4, we can see each group contains K residual distilling blocks(RDBs)

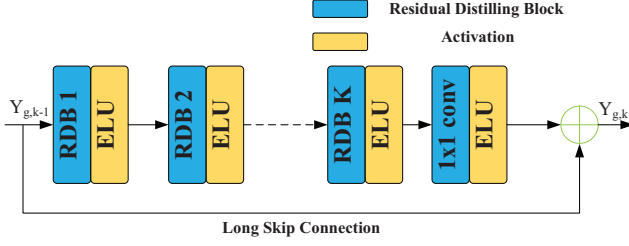


Fig. 4: Residual Distilling Group(RDG).

and one long skip connection(LSC). Such our structure can achieve high performance in image super resolution with a general number of convolution layers.

With all of the above, a RDG in g -th group is represented as

$$Y_g = F_g(Y_{g-1}) + Y_{g-1} \quad (6)$$

$$= F_g(F_{g-1}(\dots F_1(Y_0) \dots)) + Y_{g-1}, \quad (7)$$

where F_g denotes the function of g -th RDG. F_{g-1} and F_g are the input and output of g -th RDG. Unlimited use of the residual distilling will increase the number of channels by a very large amount. Therefore, we set a 1×1 convolution with ELU [16] to reduce the number of channels, but it also can combine the fused distillation features together. Finally, when g is G , we have the output of RDGs

$$Y_{RDGs} = Y_G, \quad (8)$$

where Y_G denotes the output of G -th RDG.

2.3. Residual Distilling Block

The LR images have abundant low frequency information, except high frequency information the HR images only have. Therefore, we need to extract LR information and generate high frequency information. From the perspective of feature sharing of learning, [17] found that the connection in residual learning is an effective way to eliminate the phenomenon of disappearing gradients in deep networks. Inspired by the recent success of by [17] on ImageNet, we design residual distilling as basic convolution in each RDB, that is, when the channel performs the residual operation, it simultaneously distills out the new channel. The channel operated by the residual operation, retains the input information as much as possible and the new distilled channel contains the useful features which is conducive to generate high frequency information. The residual distilling inherits the advantages of ResNet [6] and distilled efficient information, to achieve an effective reuse and re-exploitation.

For intuitive understanding, as shown in Fig.5, lets D_i denotes the feature map dimensions of the i -th layers. In this way, the relationship of the convolution layers can be expressed as:

$$D_{i+1} - D_i = d, \quad (9)$$

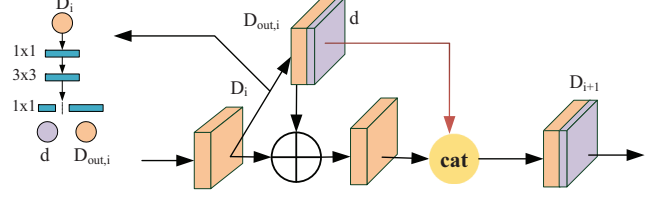


Fig. 5: Residual Distilling Block(RDB).

where d denotes the channel that is distilled out between $(i + 1)$ -th layer and i -th layer. The number of D_i dimensions perform residual operation, and d dimensions perform cat operation. The whole process can be expressed as:

$$[D_{out,i}, d] = F_{rd}(D_i), \quad (10)$$

$$D_{i+1} = F_{concat}(D_{out,i} + D_i, d), \quad (11)$$

where $[D_{out,i}, d]$ are output of D_i by convolutional function and F_{rd} denotes residual distilling function in Fig.5 left, and F_{concat} represents concatenation operation. The dimensions of $D_{out,i}$ is same as D_i . Through this process, local residual information have been extracted by residual operation, and the net still remains a distilled path to learn new features flexibility. As we all know, high resolution to low resolution is a process of information degradation. Therefore, residual distilling helps the neural network extract the useful features through potential information.

As shown in Fig.4, we stack RDBs in one RDG with one long connection. Too deep a network can cause the learned features to disappear. We design a long memory connection to allow the network reserve information about the previous block. We stack K residual distilling blocks(RDB) in each RDG. So $Y_{g,k}$, the k -th residual distilling block in g -th RDG, can be expressed as

$$Y_{g,k} = F_{RDB,k}(D_k) \quad (12)$$

$$= F_{RDB,k}(F_{RDB,k-1}(\dots F_{RDB,1}(D_1) \dots)), \quad (13)$$

where $F_{RDB,K}$ represents the k -th RDB function. The residual distilling block is simple, lightweight and accurate. Finally, we can get Y_g , the output of g -th RDG

$$F_g(Y_{g-1}) = F_p(Y_{g,K}), \quad (14)$$

$$Y_g = F_g(Y_{g-1}) + Y_{g-1}, \quad (15)$$

where F_p denotes the compression using 1×1 convolution with ELU, and $Y_{g,K}$ is the output of g -th RDG when k is K .

2.4. Image Reconstruction

As discussed in Session 2.3, the output Y_0 and Y_{RDGs} of the previous network represent global residual information and

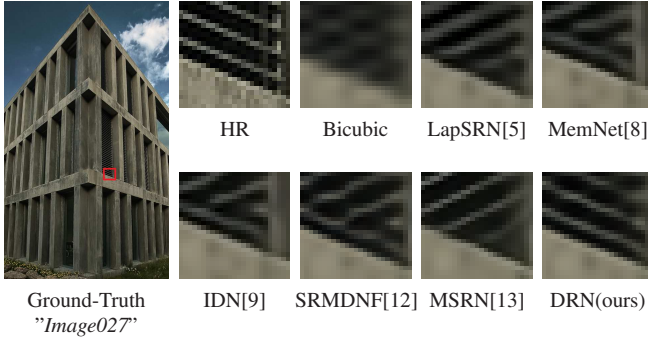


Fig. 6: Subjective quality assessment for $3\times$ upscaling on the general image: *Image027* from Urban100.

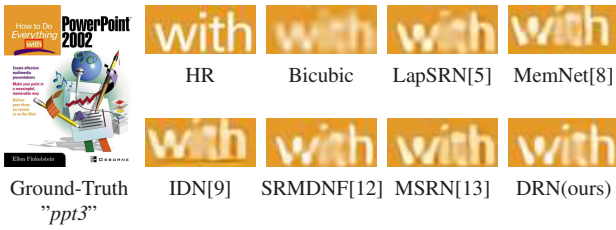


Fig. 7: Subjective quality assessment for $4\times$ upscaling on the general image: *ppt3* from Set14.

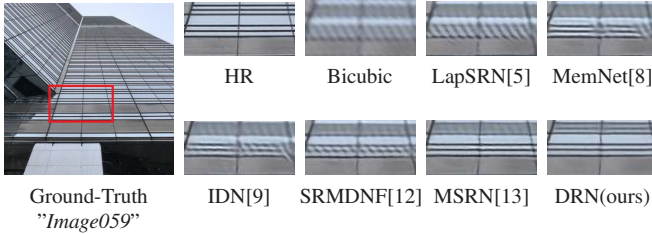


Fig. 8: Subjective quality assessment for $4\times$ upscaling on the general image: *Image059* from Urban100.

deep information respectively. Send the result Y_{DF} of the two additions to the upsampling module.

There are several methods to upscaling modules, such as deconvolution layer, nearest-neighbor upsampling convolution and pixelshuffle proposed by ESPCN [14]. However, with the upscaling factor increasing, the network will have some uncertain training problems. The weight of the deconvolution will change with the network training. Furthermore, these methods cant work on odd upscaling factors(e.g. $x3$, $x5$). Based on the above situation, we choose pixelshuffle as upscaling module due to the best performance. Detailed parameters of pixelshuffle are in Table 1.

2.5. Loss function

There are many loss functions available in the super-resolution field, such as mean square error(MSE) [1, 3, 18],

Table 1: Detailed configuration information about the reconstruction structure.

Laye name	Input channel	Output channel
conv input	C	$C\times M\times M$
PixelShuffle($\times M$)	$C\times M\times M$	C
conv output	C	3

Table 2: Quantitative comparison of results with or without RDB on Set5($3\times$) at 100th epoch.

Methods	RDBs	No RDBs	DBN+
PSNR on Set5($3\times$)	33.98	33.83	34.35

mean absolute loss [5, 7], perceptual and adversarial loss [15]. With the MSE loss, the neural networks generate images that are not in line with human vision [5], so we optimize the model with MAE that is formulated as follows:

$$l_{MAE} = \frac{1}{N} \sum_{i=1}^N \|I_i - \hat{I}_i\|_1 \quad (16)$$

where N denotes the number of training samples in each batch. I_i is the reconstructed HR image. \hat{I}_i denotes the ground truth HR image respectively. We also make a comparison of the results of using MAE and MSE respectively, as shown in Fig.??.

3. EXPERIMENTAL RESULTS

3.1. Implementation Details

In the proposed networks, we set 3×3 as the size of all convolutional layers with one padding and one striding except convolutional layers of local and global feature fusion. The filter size of local and global feature fusion is 1×1 with no padding and one striding. Low-level feature extraction layers and feature fusion layers have 64 filters. The number of RDBs K is 9, and the number of RDGs G is 6. In RD, the number of distilled filters d is 8. We treat the network with 256 original filters in each RDB as DRN+. Other layers in each RDB are followed by the exponential linear unit(ELU [16]) with parameter 0.2. The SR results are evaluated with PSNR and SSIM [19]. We train our model with ADAM optimizer [20] with MAE loss by setting $\beta_1=0.9$, $\beta_2=0.999$ and $\epsilon=10^{-8}$. The learning rate is 10^{-4} and halve at each 200 epochs. We trained DRN and DRN+ for about 800 and 300 epochs respectively.

3.2. Datasets

By following many existing image SR methods [7, 13], we use 800 training images of DIV2K dataset [21] as training set and five standard benchmark dataset: Set5 [22], Set14 [23],

Table 3: Benchmark results of state-of-the-art SR methods: Average PSNR/SSIM/IFC for $2\times$, $3\times$, and $4\times$ upscaling. The bold figures indicate the best performance.

Dataset	Scale	Bicubic	A+ [2]	VDSR [3]	DRCN [4]	LapSRN [5]	IDN [9]	SRMDNF [12]	MSRN [13]	DRN(ours)	DRN+(ours)
Set5	$\times 2$	33.66/0.9300	36.60/0.9542	37.53/0.9583	37.63/0.9584	37.52/0.9581	37.83/0.9600	37.79/0.9601	38.08/0.9605	38.06/0.9607	38.18/0.9612
	$\times 3$	30.39/0.8688	32.63/0.9085	33.66/0.9201	33.82/0.9215	33.82/0.9207	34.11/0.9253	24.12/0.9254	34.38/0.9262	34.45/0.9274	34.68/0.9293
	$\times 4$	28.42/0.8104	30.33/0.8565	31.35/0.8838	31.53/0.8854	31.54/0.8852	31.82/0.8903	31.96/0.8925	32.07/0.8903	32.27/0.8964	32.49/0.8985
Set14	$\times 2$	30.24/0.8688	32.42/0.9059	33.03/0.9124	33.04/0.9118	33.08/0.9124	33.32/0.9159	33.30/0.9148	33.74/0.9170	33.64/0.9179	33.85/0.9193
	$\times 3$	27.55/0.7742	29.25/0.8194	29.77/0.8314	29.76/0.831	29.87/0.8325	29.99/0.8354	30.04/0.8382	30.34/0.8395	30.30/0.8664	30.57/0.8466
	$\times 4$	26.00/0.7027	27.44/0.7450	28.01/0.7674	28.02/0.7670	28.19/0.7700	28.25/0.7730	28.35/0.7787	28.60/0.7751	28.69/0.7839	28.83/0.7872
BSDB100	$\times 2$	29.56/0.8431	31.24/0.8870	31.90/0.8960	31.85/0.8942	31.80/0.8952	32.08/0.8985	32.05/0.8985	32.23/0.9013	32.23/0.9001	32.32/0.9013
	$\times 3$	27.21/0.7385	26.05/0.8019	28.82/0.7976	28.80/0.7963	28.82/0.7980	28.95/0.8013	28.97/0.8025	29.08/0.8554	29.12/0.8055	29.26/0.8090
	$\times 4$	25.96/0.6675	26.83/0.6999	27.29/0.7251	27.23/0.7232	27.32/0.7284	27.41/0.7297	27.49/0.7337	27.52/0.7273	27.65/0.7380	27.72/0.7403
Urban100	$\times 2$	26.88/0.8403	29.25/0.8955	30.76/0.9140	30.75/0.9133	30.41/0.9103	31.27/0.9196	31.33/0.9204	32.22/0.9326	32.22/0.9288	32.65/0.9329
	$\times 3$	24.46/0.7349	26.05/0.8019	27.14/0.8279	27.15/0.8276	27.07/0.8275	27.42/0.8359	27.57/0.8398	28.08/0.8554	28.18/0.8520	28.73/0.8627
	$\times 4$	23.14/0.6577	24.34/0.7211	25.18/0.7524	25.14/0.7510	25.21/0.7562	25.41/0.7632	25.68/0.7731	26.04/0.7896	26.26/0.7903	26.54/0.7982
Manga109	$\times 2$	30.82/0.9332	35.37/0.9663	37.22/0.9729	37.63/0.9723	37.27/0.9855	38.02/0.9749	38.07/0.9761	38.82/0.9868	38.75/0.9773	38.94/0.9779
	$\times 3$	26.96/0.8555	29.93/0.9089	32.01/0.9310	32.31/0.9328	32.21/0.9318	32.79/0.9391	33.00/0.9403	33.44/0.9427	33.78/0.9455	34.21/0.9486
	$\times 4$	24.91/0.7826	27.03/0.8439	28.83/0.8809	28.98/0.8816	29.09/0.8845	29.41/0.8936	30.09/0.9024	30.17/0.9034	30.87/0.9121	31.16/0.9157

Urban100 [24], BSDB100 [25] and Manga109 [26] as testing set. We set the batchsize to 16. The size of the input image is 48×48 . Instead of transforming the RGB patches into a YCbCr space, we use 3 channels images information from the RGB patches in order to keep the images real.

3.3. Comparisons with state-of-the-arts

We compare our method with 10 state-of-the-art methods: A+ [2], SRCNN [1], FSRCNN [18], VDSR [3], DRCN [4], LapSRN [5], IDN [9], SRMDNF [12], EDSR [7] and MSRN [13]. We also use self-ensemble [27] to improve our models.

Table 3 shows quantitative comparison for $\times 2$, $\times 3$ and $\times 4$ SR. Compared with previous methods, our DRN+ performs the best on most datasets with all scaling factors. Even with 64 filters, our DRN is also better than other comparison methods on most datasets. Table 2 shows ablation test on RDBs. The model with RDBs has a great performance, and DBN+ has a better performance. In Fig.1, Fig.6, Fig.7 and Fig.8 we present visual performance on different datasets with different upscaling factors. Fig.1 shows visual comparison on scale $\times 4$. For image "Image075", we observe that most methods can't recover texture on the windows. In contrast, our DRN can better alleviate blurring artifacts and recover details consistent with the Groundtruth. In Fig.6 we observe that the lines of "Image027" recovered by most methods don't correspond to Groundtruth images well. However, the DRN our proposed have accurately recovered the lines. Fig.7 showing "ppt3", although most methods have different degrees of blurring on the word "with", the DRN accurately removes the blurs in the picture that people can recognize that the word is "with". In Fig.8 most methods don't recover lines of windows in "Image059" that inconsistent with Groundtruth image, our DRN accurately restores the lines and removes the blur almost.

We also compared the trade-offs between performance and network parameters from DRN networks and existing networks. Fig. 2 shows the PSNR performance versus number of parameters, where the results are evaluated with Set5 dataset for $4\times$ upscaling factor. We can see our DRN network is better than a relatively small models. In addition, the DRN+ achieves higher performance with 54% fewer parameters compared with EDSR. These comparisons show that our model has a better trade-off between performance and model size.

4. CONCLUSION

In this paper, we propose a simple and efficient distilling with residual network(DRN) for SISIR, which is better than most of the state-of-the-art methods and has fewer parameters. Based on residual distilling(RD), the DRN inherits the advantages of the dense residue and connection paths, to achieve an effective reuse and re-exploitation. Our DRN and DRN+ have better tradeoff between model size and performance. In the future, we will apply this model to other areas to such as de-raining, dehazing, and denoising.

5. REFERENCES

- [1] Chao Dong, Chen Change Loy, Kaiming He, and Xiaoou Tang, "Learning a deep convolutional network for image super-resolution," in *ECCV*. Springer, 2014, pp. 184–199.
- [2] Radu Timofte, Vincent De Smet, and Luc Van Gool, "A+: Adjusted anchored neighborhood regression for fast super-resolution," in *ACCV*. Springer, 2014, pp. 111–126.

- [3] Jiwon Kim, Jung Kwon Lee, and Kyoung Mu Lee, “Accurate image super-resolution using very deep convolutional networks,” in *CVPR*, 2016, pp. 1646–1654.
- [4] Jiwon Kim, Jung Kwon Lee, and Kyoung Mu Lee, “Deeply-recursive convolutional network for image super-resolution,” in *CVPR*, 2016, pp. 1637–1645.
- [5] Wei-Sheng Lai, Jia-Bin Huang, Narendra Ahuja, and Ming-Hsuan Yang, “Deep laplacian pyramid networks for fast and accurate super-resolution,” in *CVPR*, 2017, pp. 5835–5843.
- [6] Kaiming He, Xiangyu Zhang, Shaoqing Ren, and Jian Sun, “Deep residual learning for image recognition,” in *CVPR*, 2016, pp. 770–778.
- [7] Bee Lim, Sanghyun Son, Heewon Kim, Seungjun Nah, and Kyoung Mu Lee, “Enhanced deep residual networks for single image super-resolution,” in *CVPRW*, 2017, pp. 1132–1140.
- [8] Ying Tai, Jian Yang, Xiaoming Liu, and Chunyan Xu, “Memnet: A persistent memory network for image restoration,” in *CVPR*, 2017, pp. 4539–4547.
- [9] Zheng Hui, Xiumei Wang, and Xinbo Gao, “Fast and accurate single image super-resolution via information distillation network,” in *CVPR*, 2018, pp. 723–731.
- [10] Yulun Zhang, Yapeng Tian, Yu Kong, Bineng Zhong, and Yun Fu, “Residual dense network for image super-resolution,” in *CVPR*, 2018.
- [11] Yulun Zhang, Kunpeng Li, Kai Li, Lichen Wang, Bineng Zhong, and Yun Fu, “Image super-resolution using very deep residual channel attention networks,” *arXiv preprint arXiv:1807.02758*, 2018.
- [12] Kai Zhang, Wangmeng Zuo, and Lei Zhang, “Learning a single convolutional super-resolution network for multiple degradations,” in *CVPR*, 2018, vol. 6.
- [13] Juncheng Li, Faming Fang, Kangfu Mei, and Guixu Zhang, “Multi-scale residual network for image super-resolution,” in *ECCV*, 2018, pp. 517–532.
- [14] Wenzhe Shi, Jose Caballero, Ferenc Huszár, Johannes Totz, Andrew P Aitken, Rob Bishop, Daniel Rueckert, and Zehan Wang, “Real-time single image and video super-resolution using an efficient sub-pixel convolutional neural network,” .
- [15] Christian Ledig, Lucas Theis, Ferenc Huszár, Jose Caballero, Andrew Cunningham, Alejandro Acosta, Andrew P Aitken, Alykhan Tejani, Johannes Totz, Zehan Wang, et al., “Photo-realistic single image super-resolution using a generative adversarial network,” in *CVPR*, 2017, vol. 2, p. 4.
- [16] Djork-Arné Clevert, Thomas Unterthiner, and Sepp Hochreiter, “Fast and accurate deep network learning by exponential linear units (elus),” *arXiv preprint arXiv:1511.07289*, 2015.
- [17] Yunpeng Chen, Jianan Li, Huaxin Xiao, Xiaojie Jin, Shuicheng Yan, and Jiashi Feng, “Dual path networks,” in *NeurIPS*, 2017, pp. 4467–4475.
- [18] Chao Dong, Chen Change Loy, and Xiaoou Tang, “Accelerating the super-resolution convolutional neural network,” in *ECCV*. Springer, 2016, pp. 391–407.
- [19] Zhou Wang, Alan C Bovik, Hamid R Sheikh, and Eero P Simoncelli, “Image quality assessment: from error visibility to structural similarity,” *IEEE Transactions on Image Processing*, vol. 13, no. 4, pp. 600–612, 2004.
- [20] D Kinga and J Ba Adam, “A method for stochastic optimization,” in *ICLR*, 2015, vol. 5.
- [21] Radu Timofte, Eirikur Agustsson, Luc Van Gool, Ming-Hsuan Yang, Lei Zhang, Bee Lim, Sanghyun Son, Heewon Kim, Seungjun Nah, Kyoung Mu Lee, et al., “Ntire 2017 challenge on single image super-resolution: Methods and results,” in *CVPRW*. IEEE, 2017, pp. 1110–1121.
- [22] Marco Bevilacqua, Aline Roumy, Christine Guillemot, and Marie Line Alberi-Morel, “Low-complexity single-image super-resolution based on nonnegative neighbor embedding,” 2012.
- [23] Roman Zeyde, Michael Elad, and Matan Protter, “On single image scale-up using sparse-representations,” in *International Conference on Curves and Surfaces*. Springer, 2010, pp. 711–730.
- [24] Jia-Bin Huang, Abhishek Singh, and Narendra Ahuja, “Single image super-resolution from transformed self-exemplars,” in *CVPR*, 2015, pp. 5197–5206.
- [25] David Martin, Charless Fowlkes, Doron Tal, and Jitendra Malik, “A database of human segmented natural images and its application to evaluating segmentation algorithms and measuring ecological statistics,” in *ICCV*. IEEE, 2001, vol. 2, pp. 416–423.
- [26] Yusuke Matsui, Kota Ito, Yuji Aramaki, Azuma Fujimoto, Toru Ogawa, Toshihiko Yamasaki, and Kiyoharu Aizawa, “Sketch-based manga retrieval using manga109 dataset,” *Multimedia Tools and Applications*, vol. 76, no. 20, pp. 21811–21838, 2017.
- [27] Radu Timofte, Rasmus Rothe, and Luc Van Gool, “Seven ways to improve example-based single image super resolution,” in *CVPR*, 2016, pp. 1865–1873.

